Comparison of Two Novel Integral Equation Approaches for Lossy Conductor Modeling

Martijn Huynen, Michiel Gossye, Daniël De Zutter, Hendrik Rogier and Dries Vande Ginste
Electromagnetics Group/IDLab, Department of Information Technology, Ghent University/imec
Gent, Belgium
martijn.huynen@ugent.be

***Abstract*—In this paper, we take a closer look at two novel boundary integral equation methods that are ideally suitable for modeling good but lossy conductors. The first method leverages the Calderón identities to precondition the homogeneous Poincaré-Steklov operator for high dielectric contrast materials. The second technique constructs an alternative formulation of the Poincaré-Steklov operator based on the eigenfunctions of the volume that avoids the numerical integration of the Green's function in the conductive medium. Through numerical examples and performance comparison, the applicability of both single-source methods to model realistic conductors is demonstrated, illustrating their capability in characterizing 3-D interconnects.**

***Index Terms*—boundary integral equation (BIE), Calderón preconditioner, 3-D surface admittance**

I. Introduction

Boundary integral equations (BIEs) are a common choice to electromagnetically model homogeneous materials in free space and/or layered background media. This is mainly due to the automatic inclusion of the Sommerfeld radiation condition through the Green's function and the reduced number of unknowns as only the boundary surface demands discretization, making them ideal candidates for modeling (3-D) interconnect structures. These advantages come at the cost of the dense nature of the system matrix and the increased complexity in the calculation of the matrix elements.

Widely-used BIE methods such as the electric field integral equation (EFIE) and the Poggio-Miller-Chan-Harrington-Wu-Tsai (PMCHWT) formulation for the modeling of perfect electric conductors (PEC) and dielectric materials, respectively, additionally suffer from low-frequency and dense-mesh breakdown after discretization as they depend on the electric field integral operator, $\mathcal{T}$, an unbounded and ill-posed operator. These conditioning problems can be mitigated through the application of Calderón preconditioners [1], [2].

Unfortunately, when modeling materials exhibiting high dielectric contrast (HDC) with respect to the background medium, some (new) challenges arise. Firstly, the previously alleviated conditioning problems of the preconditioned PMCHWT formulation are resurrected and need to be tackled once more. Secondly, the calculation of the matrix elements inside the medium becomes much more involved if the complex permittivity has a strong imaginary dielectric component, as is the case for good conductors [3].

The first method we explore is a Calderón preconditioned single-source BIE that focuses on the first hurdle, i.e., the conditioning problems. To achieve this, a Poincaré-Steklov (PS) operator $\mathcal{P}$ that maps the tangential electric field onto the tangential magnetic field on the boundary surface is introduced. After proper discretization, the resulting ill-conditioned matrix equations are regularized by exploiting the stabilizing effect of the $\mathcal{T}$ operator on the PS operator [4].

The second technique we examine, focuses on the difficulty of numerically integrating the Green's function inside highly conductive media. Instead of employing advanced but computationally costly methods to compute these integrals with tolerable accuracy, a differential surface admittance (DSA) operator $\mathcal{Y}$ is introduced that avoids these computations altogether. Instead, it exploits the eigenfunctions of a cavity with the same shape as the conductive volume to construct $\mathcal{Y}$, i.e., the difference between two PS operators, leading to an alternative single-source BIE, suitable for lossy conductor modeling [5].

II. A Calderón preconditioner for HDC media

Consider a bounded volume V with boundary surface Γ filled with a homogeneous materials with (complex) permittivity and permeability ϵ and μ, respectively, embedded in a homogeneous unbounded background medium V_0, characterized by its permittivity and permeability ϵ_0 and μ_0. We now replace the material inside V by the background medium and impose a magnetic surface current density $\mathbf{m}_s$ on Γ in such a way that the field distribution outside V remains unchanged. This leads to the following set of equations that fully describe the fields inside V_0:

$$\begin{cases} \left(\mathcal{K}_0 + \frac{1}{2}\right)\mathbf{m}_s + \hat{\mathbf{n}} \times \mathbf{e} = \hat{\mathbf{n}} \times \mathbf{e}^i \\ \frac{1}{Z_0}\mathcal{T}_0\mathbf{m}_s + \mathcal{P}\left(\hat{\mathbf{n}} \times \mathbf{e}\right) = -\hat{\mathbf{n}} \times \mathbf{h}^i, \end{cases} \tag{1}$$

with $\hat{\mathbf{n}}$ the outward pointing normal of V, $Z_0 = \sqrt{\mu_0/\epsilon_0}$, $\mathbf{e}^i$ and $\mathbf{h}^i$ the impinging fields and $\mathcal{K}_0$ the magnetic field integral operator where the subscript 0 emphasizes that it is calculated utilizing the material properties of the background medium. The PS operator $\mathcal{P}$ can be computed as:

$$\mathcal{P} = \frac{1}{Z}\mathcal{T}^{-1}\left(\mathcal{K} + \frac{1}{2}\right), \tag{2}$$

where Z, $\mathcal{T}$ and $\mathcal{K}$ are now computed based on the material parameters ϵ and μ. Discretizing (1) in its current form leads to an ill-conditioned matrix. Multiplying the second equation in (1) on the left by $-Z\mathcal{T}$, alleviates this conditioning problem.

It can be shown [4] that the accumulation points of the eigenvalues of the system matrix are $1/2 \pm j/2\sqrt{\epsilon_0/\epsilon}$ and $1/2 \pm j/2\sqrt{\mu/\mu_0}$. Consequently, the formulation is well-posed and bounded for lossy conductors and other HDC materials and low-frequency and dense-mesh breakdown are averted. A dual formulation that exhibits the same advantageous properties for high magnetic contrast materials has also been developed [6].

III. A 3-D Differential Surface Admittance Operator

Assume the same configuration as before (with the added constraint of no magnetic contrast) but this time we impose an electric surface current density $\mathbf{j}_s$ instead of $\mathbf{m}_s$ when applying the equivalence principle. The PS operator for the original situation remains unchanged but now we define an additional PS operator in the equivalent case: $\hat{\mathbf{n}} \times \mathbf{h}_0 = \mathcal{P}_0 (\hat{\mathbf{n}} \times \mathbf{e}_0)$ where the subscript emphasizes the replacement of the material inside by the background medium. By comparing the boundary conditions in both scenarios, one easily shows that

$$\mathbf{j}_s = \hat{\mathbf{n}} \times (\mathbf{h} - \mathbf{h}_0) = (\mathcal{P} - \mathcal{P}_0)(\hat{\mathbf{n}} \times \mathbf{e}) = \mathcal{Y}(\hat{\mathbf{n}} \times \mathbf{e}). \quad (3)$$

Instead of computing $\mathcal{Y}$ by means of the two PS operators separately through (2), it can be shown [5] that the differential surface admittance operator can be constructed directly by utilizing the magnetic eigenmodes $\mathbf{h}_\nu$ of a PEC cavity with the same shape as V:

$$\mathbf{j}_s = \mathcal{Y}(\hat{\mathbf{n}} \times \mathbf{e}) = \tau \sum_\nu \frac{K_\nu}{N_\nu^2} \left[\int_\Gamma (\hat{\mathbf{n}} \times \mathbf{e}) \cdot \mathbf{h}_\nu \right] (\hat{\mathbf{n}} \times \mathbf{h}_\nu), \quad (4)$$

with the contrast parameter $\tau = \left(k^2 - k_0^2\right)/j\omega\mu_0$, k_ν and N_ν the wavenumber and normalization constant of $\mathbf{h}_\nu$, respectively, and $K_\nu = k_\nu^2 / \left[(k_0^2 - k_\nu^2)(k^2 - k_\nu^2)\right]$.

In order to fully solve the field equations, the $\mathcal{Y}$ operator is combined with the EFIE. For the sake of avoiding its corresponding conditioning problems, the operator is substituted in the augmented EFIE formulation, which improves the conditioning through separation of the vector and scalar potential in the $\mathcal{T}$ operator by introducing an additional set of unknowns and constructing a sparse preconditioner [7].

IV. Characteristics of both methods

In this section, we briefly discuss the overall similarities and differences between both methods, which are reflected in the numerical results of Section V. Their main common point is that they are both single-source BIE formulations that employ the Poincaré-Steklov operator. This implies, among other things, that both methods exhibit internal resonances.

The main difference between both methods is their generality. The first method can be applied to arbitrary shapes, given that it functions optimally for smooth objects, while the second method, due to its reliance on eigenfunctions, is only efficiently applicable to canonical shapes, whose eigenfunctions are known analytically. An advantage of the second method is that the average mesh element size does not scale with the wavelength inside the material as no field quantities on the inside are computed directly; this is in contrast to the first method. However, the higher the dielectric contrast, the more eigenmodes need to be considered for accurate results. As the number of eigenmodes can be regulated independently from the mesh size, this does not impact the computation time for the EFIE system matrix.

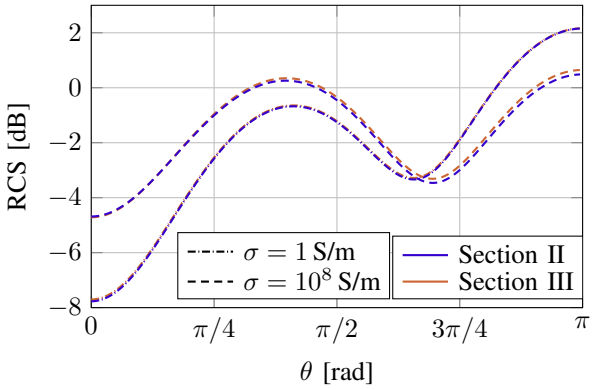

Fig. 1. Radar cross sections (RCSs) in the xz-plane of a cube with a side of 0.5 m for a plane wave propagating along the positive z-axis and linearly polarized along the x-axis at 200 MHz. The method from Section II is compared to the method described in Section III for two different values of the conductivity σ.

V. Numerical examples

In the first numerical example, we examine the performance of both methods in computing the radar cross section (RCS) for a conductive cube with a side length of 0.5 m when illuminated by a plane wave propagating along the positive z-axis and polarized in the x-direction at a frequency of 200 MHz. Both methods employ a surface mesh such that the sides of the cube are divided into 6 edges, which results in a total of 936 and 432 edges, respectively, as the first method uses a procedurally generated triangular mesh whereas the second method imposes a structured rectangular grid [8]. The RCS in the xz-plane is visualized in Figure 1 for a low and high conductivity of 1 S/m and 10^8 S/m. The results agree very well for all angles save for the highly conductive case, which can be attributed to the influence of the relative coarseness of the mesh for the Calderón preconditioned HDC method. The total computation time (matrix calculation, iterative solution and post-processing time) for this method amounts to around 5 minutes while the DSA based method computes the RCS within a minute.

The number of iterations required in the iterative solution of the two systems with the generalized minimal residual method within a tolerance of 10^{-10} is reported in Figure 2 for an increasing value of σ. Both methods obtain the results within a similar limited number of iterations and converge to a steady value for highly conductive materials instead of growing boundlessly. Despite the larger system matrix size for the method from Section II, it achieves a comparable convergence speed due to its more advanced preconditioner.

The second example constitutes the same scattering set-up as for the conductive cube but now the illuminated object is an

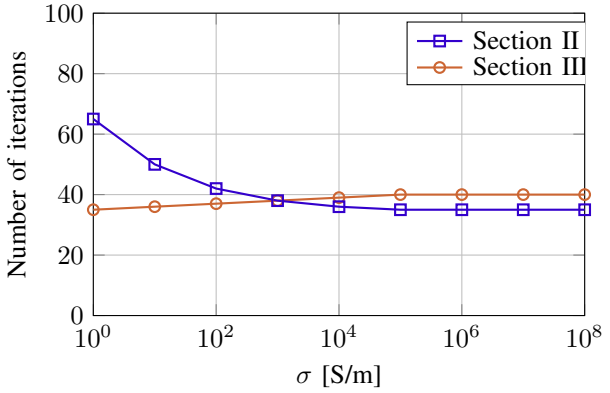

Fig. 2. Number of iterations until convergence of the two methods in computing the radar cross section of Figure 1 for increasing values of σ.

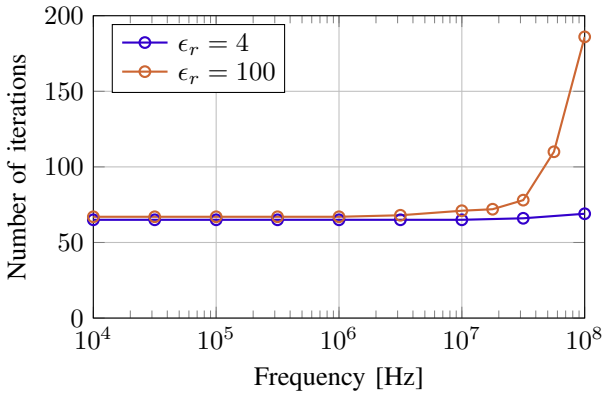

Fig. 3. Number of iterations until convergence of the Calderón preconditioned HDC method as a function of frequency for two different dielectric contrasts. The same scattering configuration as in Figure 1 is employed with the illuminated object being an ellipsoid with principal semi-axes of 0.6 m, 0.4 m and 0.2 m.

ellipsoid with principal semi-axes of 0.6 m, 0.4 m and 0.2 m, respectively. For two different dielectric contrasts, i.e., $\epsilon_r = 4$ and $\epsilon_r = 100$, the number of iterations until convergence (tolerance of 10^{-10}) for a wide range of frequencies are displayed in Figure 3 for the Calderón preconditioned HDC method. The number of iterations is limited and stable over several decades, thus demonstrating the lack of low-frequency breakdown regardless of the dielectric contrast. Only toward the highest frequency of 100 MHz does the number of iterations for the high contrast material increase due to the proximity of internal resonances.

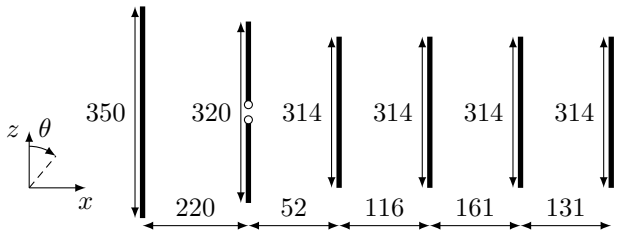

Fig. 4. Yagi-Uda antenna with one reflector and four directors intended for operation in the ISM band centered around 434 MHz. All dimensions are given in mm. The radius r of all elements is 2 mm.

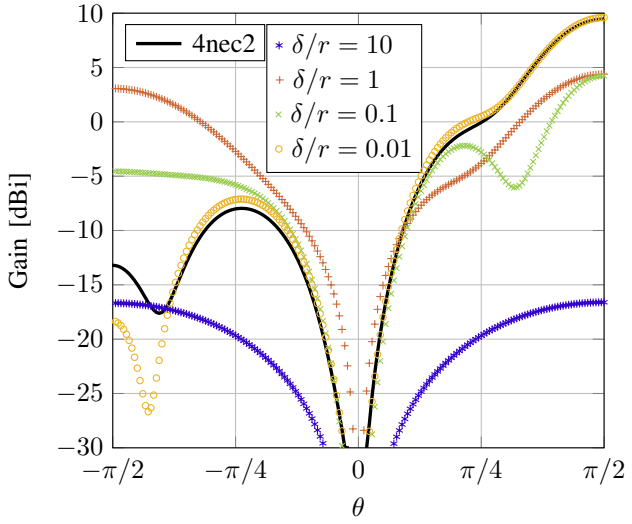

Fig. 5. Gain of the Yagi-Uda antenna depicted in Figure 4 for increasing conductivity. The PEC reference result is obtained through 4nec2 [9].

In the third example, we study the influence of the conductivity on the gain pattern of the Yagi-Uda antenna shown in Figure 4 by means of the DSA operator. It is designed for operation at 434 MHz, the center frequency of an industrial, scientific and medical (ISM) band. The radius of the various elements constituting the antenna is 2 mm and the other dimensions are annotated on the figure. Figure 5 shows the gain of this antenna for four different conductivity values, expressed as the ratio between the skin depth and the radius. For the lowest value, the gain pattern resembles that of a very ineffective dipole, i.e., the reflector and directors appear transparent due to their poor conductivity. Once the skin effect starts to kick in, the overall gain increases and the difference between the forward and backward gain grows as all the elements in the antenna start to exert their influence. For the highest conductivity, the result simulated by the DSA operator coincides with the 4nec2 reference result [9] for most angles, except for the backward gain, where the thin-wire approximation of the reference result overestimates the backside lobe.

VI. Conclusion

Two different, novel boundary equation formulations that are particularly equipped for the inclusion of lossy conductor media are presented and discussed in this paper. The first method is a single-source BIE formulation that through the use of the Calderón identities, regularizes the Poincaré-Steklov operator, resulting in favorable spectral properties for high dielectric contrast media. The second single-source method, which relies on the differential surface admittance operator, exhibits better accuracy and speed on the presented examples but is in its most efficient form limited to geometries of canonical shapes. Nevertheless, both methods are demonstrated to be aptly capable of accurate modeling for various applications over a wide variety of materials and frequencies.

Future research is still required for the presented methods to be widely deployable in interconnect modeling. Scalability and inclusion of layered media are examples of such vital requirements for both techniques. Another promising avenue that warrants pursuing is the combination of both methods by applying the Calderón-based preconditioning to the second method or by applying a domain decomposition that assigns parts of interconnects to either technique, leveraging the strength of the two methods to their full potential.

REFERENCES

[1] F. P. Andriulli, K. Cools, H. Bagči, F. Olyslager, A. Buffa, S. Christiansen, E. Michielssen, "A Multiplicative Calderón Preconditioner for the Electric Field Integral Equation," *IEEE Transactions on Antennas and Propagation*, vol. 56, no. 8, August 2008, pp. 2398–2412.

[2] K. Cools, F. P. Andriulli, E. Michielssen, "A Calderón Multiplicative Preconditioner for the PMCHWT Integral Equation," *IEEE Transactions on Antennas and Propagation*, vol. 59, no. 12, December 2011, pp. 4579–4587.

[3] J. Peeters, I. Bogaert, D. De Zutter, "Calculation of MoM Interaction Integrals in Highly Conductive Media," *IEEE Transactions on Antennas and Propagation*, vol. 60, no. 2, February 2012, pp. 930–940.

[4] M. Gossye, M. Huynen, D. Vande Ginste, D. De Zutter, H. Rogier, "A Calderón Preconditioner for High Dielectric Contrast Media," *IEEE Transactions on Antennas and Propagation*, vol. 66, no. 2, February 2018, pp. 808–818.

[5] M. Huynen, M. Gossye, D. De Zutter, D. Vande Ginste, "A 3-D Differential Surface Admittance Operator for Lossy Dipole Antenna Analysis," *IEEE Antennas Wireless Propagation Letters*, vol. 16, 2017, pp. 1052–1055.

[6] M. Gossye, D. Vande Ginste, H. Rogier, "Electromagnetic modeling of high magnetic contrast media using Calderón preconditioning," *Computers & Mathematics with Applications*, vol. 77, no. 6, March 2019, pp. 1626–1638.

[7] Z.-G. Qian, W. C. Chew, "Fast Full-Wave Surface Integral Equation Solver for Multiscale Structure Modeling," *IEEE Transactions on Antennas and Propagation*, vol. 57, no. 11, November 2009, pp. 3594–3601.

[8] M. Huynen, K. Y. Kapusuz, X. Sun, G. Van der Plas, E. Beyne, D. De Zutter, D. Vande Ginste, "Entire Domain Basis Function Expansion of the Differential Surface Admittance for Efficient Broadband Characterization of Lossy Interconnects," *IEEE Transactions on Microwave Theory and Techniques*, vol. 68, no. 4, 2020, pp. 1217–1233.

[9] A. Voors, "4nec2: Antenna modeler," http://www.qsl.net/4nec2/, 2015.